DFT+U Optical Features of Thermochromic VO_2: A Powerful Tool Towards Functional Daytime Radiative Passive Cooling Implementation

Costanza Borghesi[1,2(✉)], Claudia Fabiani[3,4], Anna Laura Pisello[3,4], and Giacomo Giorgi[1,2,5]

[1] Department of Civil and Environmental Engineering (DICA), University of Perugia, Via G. Duranti 93, 06125 Perugia, Italy
costanza.borghesi@dottorandi.unipg.it
[2] CIRIAF - Interuniversity Research Centre, University of Perugia, Perugia, Italy
[3] Department of Engineering, Università degli Studi di Perugia, Via G. Duranti 93, 06125 Perugia, Italy
[4] EAPLAP@CIRIAF - Interuniversity Research Centre, University of Perugia, Perugia, Italy
[5] CNR-SCITEC, 06123 Perugia, Italy

Abstract. The structural, electronic and optical properties of both monoclinic and rutile polymorphs of vanadium dioxide, VO_2, have been determined by means of first-principles calculations based on semiempirical DFT+U method. The outcome shows that the Hubbard U scheme provides bandgap values consistent with previously reported experimental ones. The simulated optical properties for the high-temperature rutile polymorph correctly reproduce the metallic behaviour of the system. It is interesting to note that at low temperatures, the VO_2 monoclinic structure is more transparent under infrared light irradiation, while the rutile phase blocks the same IR light, as demonstrated by the simulated optical reflectance and absorption coefficient. This work aims to provide the readers with a comprehensive understanding of the complex chemistry of VO_2, paving the way to future studies addressing the doping effect on the optical and thermal behaviour of the system in view of the application of such material in devices for radiative cooling.

Keywords: Thermochromic materials · Density Functional Theory (DFT) · Hubbard U · Daytime radiative passive cooling

1 Introduction

Together with photochromic [1,2], hydrochromic [3], and electrochromic [4,5], thermochromic materials [6] are gaining enormous attention in the technological landscape. The interest towards this latter class of compounds stems from their

© The Author(s), under exclusive license to Springer Nature Switzerland AG 2024
O. Gervasi et al. (Eds.): ICCSA 2024 Workshops, LNCS 14823, pp. 415–426, 2024.
https://doi.org/10.1007/978-3-031-65329-2_28

unique abilities to reduce energy waste and improve indoor comfort, as response to an external natural impulse, i.e. temperature change. As consequence of such T variation indeed, these materials, largely exploited in the production of thermochromic smart windows [7] and related devices, alter their visible optical characteristics [8].

For this reason, a thorough understanding of its electronic properties at the atomistic level can aid in understanding the properties of this complex material for other applications which require enviromentally-responsive solutions, such as radiative cooling devices. Daytime radiative cooling (DRC) [9,10] is a cutting-edge technology that can be used in arid environments to address the urban heat island effect and provide passive cooling in the built environment. This technology takes advantage of the Earth's atmosphere's high transparency in the mid-infrared (MIR) wavelengths between 8 and 13 μm, also known as the "sky window" region [11] to release excess heat directly into the cold universe. Radiative coolers have remarkable potential for both local climate change mitigation and passive building cooling since they can achieve sub-ambient temperatures even during peak hours by utilizing a 3 K heat sink of the outer space. Novel models of passive daytime radiative cooling have recently been presented combining high solar reflectance with high emissivity in the atmospheric window [12], even though without deeply investigating the properties of functional materials, essential to logically develop and enhance few desired attributes which assure those devices the maximum efficiency along with wide versatility. In this regard, thermochromic materials such as VO_2 can be incorporated into a multilayered device in which the optoelectronic characteristics can be turned "on" and "off" to activate the qualities of other layers (such as the thermal emission layer's activation or deactivation) [13]. The peculiar property of thermal switch it is due to the fact that at T$\approx$ 68 °C (hereafter, T_c), the monoclinic (M1, space group $P2_1/c$) experiences a fully reversible metal-insulator phase transition (MIT), transforming into rutile-type VO_2 (R, space group $P4_2/mnm$) phase (see Fig. 1). At such temperature the MIT takes place quickly-typically in the picosecond's timescale (10^{-12} s) [14]. A lot of efforts have been spent by the community to explain the physics behind this MIT. Its occurrence is nowadays interpreted through two main competitive mechanisms: a structure-driven Peierls transition [15] or an electron-correlation driven Mott transition [16]. Several authors similarly adduce the transition to a cooperative mechanism between the two [17,18]. Our goal is to technologically exploit the fundamental thermochromic characteristic of such material (clearly associated to mentioned MIT) in order to properly regulate the emission of thermal radiation, which dissipates a significant quantity of heat connected to the incident solar energy. As consequence, the amount of energy required for cooling-related operations would massively reduce.

Before describing VO_2 application properties, however, we have to better focus on the material, describing its fundamental chemical and physical properties. Indeed, VO_2 is part of the class of the so-called *strongly correlated compounds* whose characterization has represented so far one of the most challenging fields of investigation in condensed matter physics [19]. With such terminology

we refer to those materials whose electronic behaviour (which arises from the complex chemistry of *3d* electrons in VO_2) is not properly described by standard Density Functional Theory (DFT) approaches. Polymorphism is another main feature of VO_2. Indeed, the vanadium-oxygen phase diagram displays approximately twenty stable vanadium oxide compounds, including, among the others, VO, V_6O_{13}, and V_7O_{13}. Only a very small range of partial pressures of oxygen can cause VO_2 to exist. Furthermore, over ten different types of vanadium dioxide crystalline phases have been documented [20]. These include tetragonal rutile-type VO_2 (R) ($P4_2/mnm$), monoclinic-type VO_2(M1) ($P2_1/c$), tetragonal VO_2 ($P4_2/nmc$), monoclinic VO_2 (C2/m), orthorhombic VO_2·H2O (P222), tetragonal $VO_2 \cdot 0.5H_2O$ (I4/mmm), and $V_2O_4 \cdot 2H_2O$ [14].

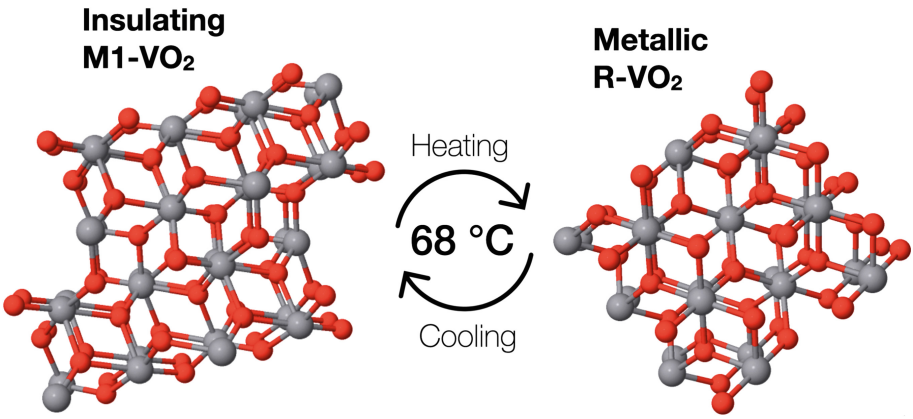

Fig. 1. Visual representation of VO_2 Metal-Insulator reversible transition at 68 °C between (left) the low temperature monoclinic (space group: $P2_1/c$) phase and (right) the high temperature rutile (space group: $P4_2/mnm$) phase.

Thus, we aim here to investigate the structural and electronic characteristics of VO_2, with a focus on optical features of M1 and R-VO_2 as prototypical investigations for future researches where we would like to address the link between the phase transition and the MIT temperature, trying to reduce it closer to room temperature (RT), thus making VO_2 more exploitable, given its potential applicability in next-generation construction materials.

Beyond the (1) high transition temperature (T_c= 68 °C) - significantly higher than RT- two other reasons motivate the fact VO_2 is not immediately employed as coatings on thermochromic materials based devices: (2) a low solar modulation efficiency (< 10%); and (3) a low luminous transmittance (∼40%) [21]. Several attempts have been made to improve them, such as element doping [22], the creation of VO_2 nanocomposites [23], the use of various substrates [24], and the alteration of structures. Element doping for VO_2 film is one of these strategies that effectively lowers T_c. It has been demonstrated that VO_2 films doped with

high valence cations, such as W^{6+}, Mo^{6+}, Ta^{5+}, Ti^{4+}, and Ru^{4+}, lower the MIT temperature [21,25]. Although its solar modulation efficiency was only 6.1%, tungsten doping has the largest MIT temperature fall-off rate among them and has been lowered to about 25 °C [26]. The optical characteristics of these films though have not significantly improved, and it is unclear how these dopants - particularly Si- affect the MIT [27]. A relevant observation is that most dopants show an upper limit in doping level to reduce the MIT temperature. In more detail, Eu^{3+}, Tb^{3+}, Nb^{5+}, P^{3+}, W^{6+}, Si^{4+}, F^{-} and Mo^{6+} are shown to produce extremely positive effects on the switching efficiency, whether Mg^{2+}, Fe^{3+}, Sb^{3+} and Zr^{4+} ions were reported to have minimal impact on the T_c as demonstrate by Wang et al. [28] In the following we report our more recent results which comprise a complete theoretical description of the electronic and optical properties of M1 and R polymorphs of VO_2, to gain insights on how this phase transition can be exploited to produce modulated optical properties. Such results represent a benchmark analysis for future investigations focusing on the doping procedure as trigger for the phase change and colour tunability.

2 Computational Details

We performed first-principles calculations in the framework of density-functional theory as implemented in the SIESTA package [29]. In particular, norm-conserving Trouillier-Martins (TM) [30] pseudopotentials for the core electrons and a triple-ζ basis set along with the generalized gradient approximation (GGA) as parametrized by Perdew-Burke-Ernzerhof (PBE) [31] for the exchange-correlation energy were employed. We have fully relaxed, lattice and ionic positions, both the structures of M1 and R-VO_2 until the maximum residual force was lower than 0.005 eV/Å, while the considered energy cutoff was of 300 Ry. Convergence in relation to the quantity of k points was thoroughly examined. Different Hubbard U [32] were tested and used to account for the electron-electron Coulomb interaction in the *3d* orbitals of V atoms.

3 Results and Discussion

The VO_2 is a monoclinic (M1) structure (shown in Fig. 2(a)) with space-group $P2_1/c$ (No. 14) at $T < T_c$. The V^{4+} ions deviate from the unit cell's center and vertex, resulting in the twist of VO_6 octahedral cages, the fundamental building blocks. The vanadium atoms tilt and dimerize to form zigzag-like chains with alternating various V-V bond lengths (see Fig. 2(b)), which is another feature specifically characterizing the M1 phase. On the other hand, the thermodynamically stable phase of VO_2 at ambient pressure and above T_c belongs to the $P4_2/mnm$ (No. 136) space group (represented in Fig. 2(c)), which has a tetragonal R structure. The tetragonal crystal cell's body center and apex are occupied by V^{4+} ions in the R-VO_2 phase. An octahedral VO_6 unit is made up of six O^{2-} ions that surround a single V^{4+} ion and vanadium atoms form equally spaced

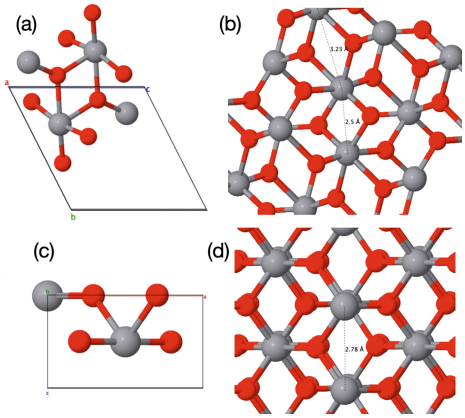

Fig. 2. DFT+U optimized crystal structure of VO_2: (a) and (c) unit cell of M1-VO_2 and R-VO_2 respectively; (b) and (d) zig-zag and linear pattern of V-V chains after metal-insulator transition (MIT). Vanadium atoms are represented with grey spheres, while red spheres are used for oxygen atoms. (Color figure online)

V-V straight chains (see Fig. 2(d)) in the c direction, while the octahedral unit creates edge-sharing chains along the c axis.

As previously mentioned, one of the relevant features of VO_2 is its strongly bound *3d* electrons. Periodic plane-wave DFT computations with standard exchange-correlation functions-like LDA or GGA-are quite successful in characterizing a wide range of materials; yet they are unable to handle systems with strong correlations. Typically, they might underestimate the band gaps and occasionally even predict a metallic ground state that is qualitatively inaccurate, such the insulating nature of M1-VO_2. The main reason is, as previously mentioned, the standard DFT failure in accounting for the correlation among *3d* V electrons. Therefore, to address this limitation and gain a better understanding of the electrical characteristics of two VO_2 phases, the present work employed the moderately computationally expensive DFT+U approach [33], which represents the electronic correlation of V-*3d* orbitals. The image below (Figs. 3(c) and 4(c)) shows the gap opening and closure due to the strong Coulomb interactions between V-*3d* electrons.

Since earlier research has demonstrated that the magnitude of effective U value, U=1.5 eV is suitable for properly describing both electronic and dynamic features of the two phases of VO_2 [34] along with its MIT temperature within the framework of the quasi-harmonic-approximation (QHA) approximation, employing this value of U, Table 1 shows the structural properties and band gaps for simulated and experimental structures. Regarding the monoclinic phase, the employed level of theory can accurately reproduce two distinct dimerized V-V bond distances: 2.50 Å and 3.23 Å in good agreement with the experimental values of 2.62 Å [35] and 3.16 Å [36]. Similarly, the optimized V-V bond length in the rutile phase is 2.78 Å, still in close agreement with the experimentally

reported value (2.85 Å) [37]. The DFT+U (U=1.5 eV) results both reproduce the insulating features of the M1 phase with a predicted bandgap (0.68 eV) perfectly in line with available experimental data [38] and the metallic behaviour of the R structure.

Table 1. DFT+U (U=1.5 eV) optimized lattice parameters, V-V bond lengths/distances and band gaps for M1 and R phase of VO_2. Experimental data are similarly reported for the sake of comparison.

Polymorph	Method	Lattice parameters (Å)	V-V distance (Å)	Bandgap (eV)
M1	DFT+U	a=4.65 b=5.47 c=5.40 α=63.0 β=90.0 γ=90.0	2.50, 3.23	0.68
	Experimental		2.62 [35], 3.16 [36]	0.67 [38]
R	DFT+U	a=4.67 b=4.67 c=2.78 α=90.0 β=90.0 γ=90.0	2.78	Metallic
	Experimental		2.85 at 360 K [37]	

To confirm the effectiveness of the selected value of U, band structures and partial density of states (PDOS) for the M and R phase of VO_2 were also computed using DFT+U (U=1.5 eV) and reported in Fig. 3(a) and Fig. 4(a), respectively. In both pictures, the zero energy is set to the Fermi energy position. The R phase metallic nature is confirmed by the DFT+U (U=1.5 eV), which, as stated before, yields an indirect band gap of 0.68 eV for the insulating M1 phase. The band dispersions around the Fermi level well reproduce the previously reported DFT findings [34]. Further proof of the distinctive characteristics of the M and R phase may be found in the partial density of states (PDOS) displayed in the right panel of Fig. 3(b) and Fig. 4(b), respectively.

The imaginary part ($\epsilon 2$) of the dielectric function in metallic species should approach infinite as photon frequency approaches zero (often referred to as the Drude tail) in accordance with Drude theory [39–41]. Since optical conductivity and $\epsilon 2$ are closely correlated, low frequencies should show a significant increase in optical conductivity. Generally, *d-d* intraband transitions and free carrier absorption are responsible for the Drude tail in VO_2. We therefore computed optical

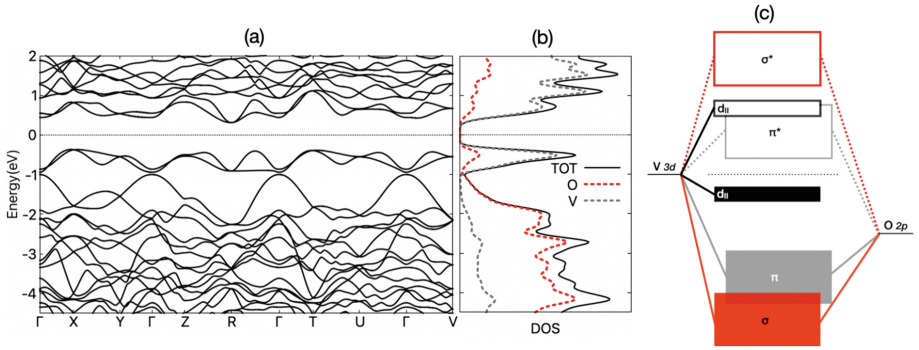

Fig. 3. DFT+U method (U=1.5 eV) calculated (a) bandstructure, and corresponding (b) density of states (DOS) along with the (c) energy-band alignment for M1-VO_2. The black dashed line represents the Fermi level.

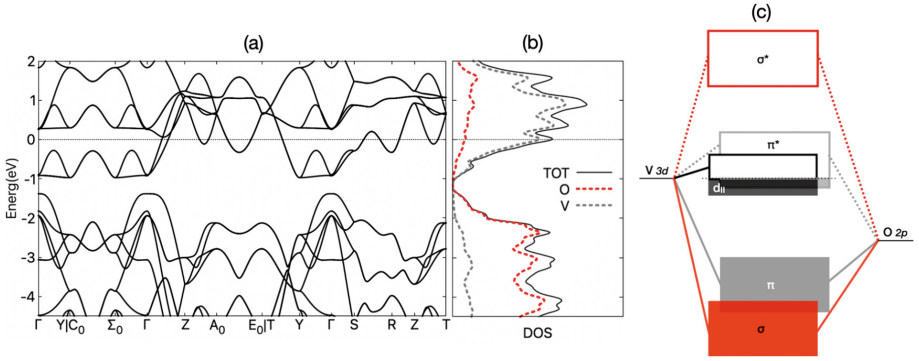

Fig. 4. DFT+U method (U=1.5 eV) calculated (a) bandstructure, and corresponding (b) density of states (DOS) along with the (c) energy-band alignment for R-VO_2. The black dashed line represents the Fermi level.

conductivity with increasing U values, finding that our optical conductivity, as determined by PBE+U calculations, reproduces correctly the Drude tail for the rutile, metallic, phase of VO_2. This is also supported by previous theoretical studies [42] where hybrid functionals are demonstrated to fail on grasping the metallic character of R-VO_2. Examining the results, we realize that the implemented U value and the Drude tail's magnitude are inversely correlated (see Fig. 5). At low frequencies, conductivity increases as the U value decreases. As frequency approaches zero, standard PBE calculations (U=0 eV) produce the largest increase in conductivity. Thus, for the metallic compounds under analysis, we conclude that the addition of the U value results in a reduction of free carrier absorption strength and *d*-*d* intraband transitions. The optical conductivity at higher energies does not show sensitive variations as function of the

U value adopted. This finding further assesses the suitability of the U value we selected for our analysis.

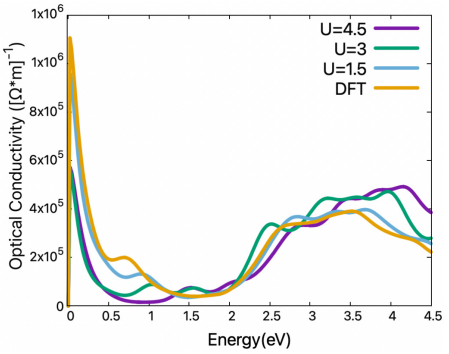

Fig. 5. DFT and DFT+U calculated optical conductivity of R-VO_2.

As previously stated, increasing temperature, VO_2 undergoes a phase transition and diffusion, allowing the material to change from an insulating to a metallic state, with consequent variation of optical properties.

Accordingly, Figs. 6, 7, 8 shows the relationship between VO_2 phase (M and R) and optical conductivity, reflectance, and absorption coefficient, respectively. In Fig. 6 the optical conductivity plot clearly indicates that R-VO_2 has high optical value around 0 eV - as expected according to the Drude model - whilst when VO_2 changes from metallic to insulating phase, the optical conductivity also decreases accordingly at frequencies close to zero. The simulated results are in good agreement with experimentally measured optical conductivity profiles found in literature [42]. The VO_2 MIT also significantly affects the optical reflectance as depicted in Fig. 7, where we observe low infrared (IR) reflectance in the insulating phase but high IR reflectance in the R metallic phase, a useful property to exploit in functional devices based on thermochromic films [43]. Finally, the absorption coefficients (reported in Fig. 8) of M1 and R-VO_2 shows that the pure M1 phase has very low absorption and reflection of IR light, whilst the pure R phase exhibits a strong absorption and reflection in the same region. These aspects clearly indicate that IR light more easily interacts with the M1 phase, but it is mostly blocked once it interacts with the R phase, an outcome in good agreement with the experimental observations and previous theoretical results [44].

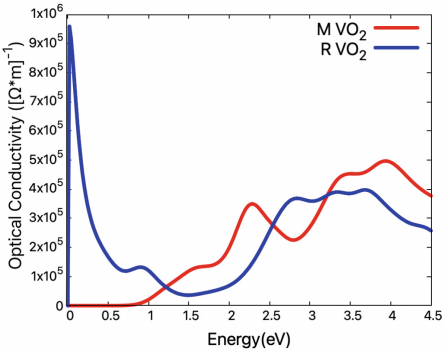

Fig. 6. DFT+U (U=1.5 eV) calculated optical conductivity of (blue) M and (red) R-VO_2. (Color figure online)

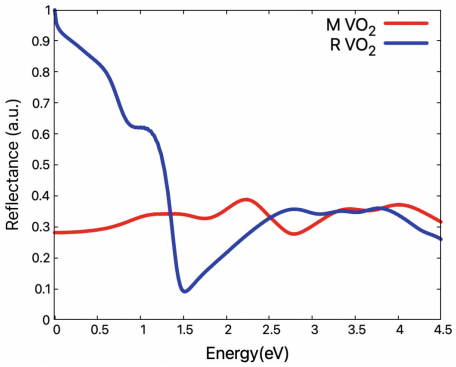

Fig. 7. DFT+U (U=1.5 eV) calculated reflectance of (blue) M and (red) R-VO_2. (Color figure online)

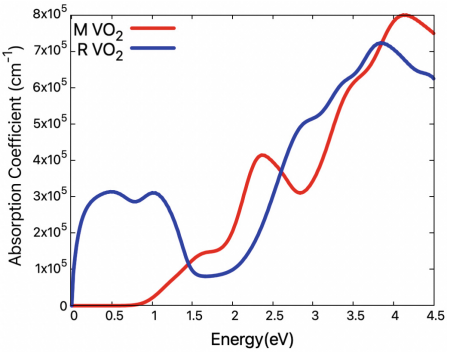

Fig. 8. DFT+U (U=1.5 eV) calculated absorption coefficient of (blue) M and (red) R-VO_2. (Color figure online)

4 Conclusions

In the present contribution the physical features of VO_2 main polymorphs, rutile and monoclinic, have been addressed in terms of their optical and electronic properties. Our results are consistent with those previously reported in literature, confirming that the DFT+U approach accurately predicts the insulating and metallic character of M1 and R phase, respectively, and further supporting the suitability of such approach for electronic structures calculation of other strongly correlated materials. Based on the obtained results, we have further noticed that increasing the U value induces a large reduction of free carrier absorption and *d*-*d* intraband transitions, therefore reducing the characteristic Drude tail for the metallic compounds. Carefully screening the Hubbard U value, we conclude that our selected one (U=1.5 eV) fairly reproduce the predicted behaviour of the two phases.

Our work paves the way towards future investigations aiming to disclose any possible relationship between VO_2 optical features and doping effects on the two polymorphs. In this framework, particular focus must be paid on the impact that do pant atoms may have in the metal-to-insulator transition temperature.

Acknowledgments. Funded by the European Research Council within the framework of the Horizon Europe Programme (ERC, HELIOS, G.A. 101041255, PI dr. A.L. Pisello). Views and opinions expressed are, however, those of the authors only and do not necessarily reflect those of the European Union or the European Research Council. Neither the European Union nor the granting authority can be held responsible for them. G.G., A.L.P. also thank the European Union - NextGenerationEU under the Italian Ministry of University and Research (MUR) National Innovation Ecosystem Grant ECS00000041 - VITALITY for funding and acknowledge Università degli Studi di Perugia and MUR for support within the project Vitality. Authors are similarly grateful to Prof. L. Latterini and her research group (Dept of Chemistry, Biology and Biotechnology, Perugia University) for the very fruitful scientific discussions.

Disclosure of Interests. The authors have no competing interests to declare that are relevant to the content of this article.

References

1. Irie, M.: Photochromism: memories and switches introduction. Chem. Rev. **100**(5), 1683–1684 (2000)
2. Dürr, H., Bouas-Laurent, H.: Photochromism: Molecules and Systems. Elsevier (2003)
3. Nandakumar, D.K., Ravi, S.K., Zhang, Y., Guo, N., Zhang, C., Tan, S.C.: A super hygroscopic hydrogel for harnessing ambient humidity for energy conservation and harvesting. Energy Environ. Sci. **11**(8), 2179–2187 (2018)
4. Mortimer, R.J.: Electrochromic materials. Chem. Soc. Rev. **26**(3), 147–156 (1997)
5. Somani, P.R., Radhakrishnan, S.: Electrochromic materials and devices: present and future. Mater. Chem. Phys. **77**(1), 117–133 (2003)

6. Kamalisarvestani, M., Saidur, R., Mekhilef, S., Javadi, F.: Performance, materials and coating technologies of thermochromic thin films on smart windows. Renew. Sustain. Energy Rev. **26**, 353–364 (2013)
7. Wang, X., Narayan, S.: Thermochromic materials for smart windows: a state-of-art review. Front. Energy Res. **9**, 800382 (2021)
8. Shen, N., et al.: Vanadium dioxide for thermochromic smart windows in ambient conditions. Mater. Today Energy **21**, 100827 (2021)
9. Ulpiani, G., Ranzi, G., Feng, J., Santamouris, M.: Expanding the applicability of daytime radiative cooling: technological developments and limitations. Energy Build. **243**, 110990 (2021)
10. Kousis, I., Pisello, A.L.: Toward the scaling up of daytime radiative coolers: a review. Adv. Opt. Mater. **11**(21), 2300123 (2023)
11. Fan, S., Raman, A.: Metamaterials for radiative sky cooling. Natl. Sci. Rev. **5**(2), 132–133 (2018)
12. Borghesi, C., et al.: Tailoring high-entropy oxides as emerging radiative materials for daytime passive cooling. Chem. Mater. **35**(24), 10384–10393 (2023)
13. Nakano, M., et al.: Infrared-sensitive electrochromic device based on VO2. Appl. Phys. Lett. **103**(15) (2013)
14. Gao, Y., et al.: Nanoceramic VO2 thermochromic smart glass: a review on progress in solution processing. Nano Energy **1**(2), 221–246 (2012)
15. Goodenough, J.B.: The two components of the crystallographic transition in VO2. J. Solid State Chem. **3**(4), 490–500 (1971)
16. Qazilbash, M.M., et al.: Mott transition in VO2 revealed by infrared spectroscopy and nano-imaging. Science **318**(5857), 1750–1753 (2007)
17. Haverkort, M.W., et al.: Orbital-assisted metal-insulator transition in VO2. Phys. Rev. Lett. **95**(19), 196404 (2005)
18. Grandi, F., Amaricci, A., Fabrizio, M.: Unraveling the Mott-Peierls intrigue in vanadium dioxide. Phys. Rev. Res. **2**(1), 013298 (2020)
19. Morosan, E., Natelson, D., Nevidomskyy, A.H., Si, Q.: Strongly correlated materials. Adv. Mater. **24**(36), 4896–4923 (2012)
20. Goodenough, J.B.: Metallic oxides. Prog. Solid State Chem. **5**, 145–399 (1971)
21. Li, S.-Y., Niklasson, G.A., Granqvist, C.-G.: Thermochromic fenestration with VO2-based materials: three challenges and how they can be met. Thin Solid Films **520**(10), 3823–3828 (2012)
22. Mlyuka, N., Niklasson, G.A., Granqvist, C.-G.: Mg doping of thermochromic VO2 films enhances the optical transmittance and decreases the metal-insulator transition temperature. Appl. Phys. lett. **95**(17) (2009)
23. Faucheu, J., Bourgeat-Lami, E., Prevot, V.: A review of vanadium dioxide as an actor of nanothermochromism: challenges and perspectives for polymer nanocomposites. Adv. Eng. Mater. **21**(2), 1800438 (2019)
24. Muraoka, Y., Ueda, Y., Hiroi, Z.: Large modification of the metal-insulator transition temperature in strained VO2 films grown on TiO2 substrates. J. Phys. Chem. Solids **63**(6–8), 965–967 (2002)
25. Chen, S., Liu, J., Wang, L., Luo, H., Gao, Y.: Unraveling mechanism on reducing thermal hysteresis width of VO2 by Ti doping: a joint experimental and theoretical study. J. Phys. Chem. C **118**(33), 18938–18944 (2014)
26. Li, B., Tian, S., Tao, H., Zhao, X.: Tungsten doped M-phase VO2 mesoporous nanocrystals with enhanced comprehensive thermochromic properties for smart windows. Ceram. Int. **45**(4), 4342–4350 (2019)

27. Liang, Z., et al.: Tungsten-doped vanadium dioxide thin films as smart windows with self-cleaning and energy-saving functions. J. Alloy. Compd. **694**, 124–131 (2017)
28. Wang, N., et al.: Terbium-doped VO2 thin films: reduced phase transition temperature and largely enhanced luminous transmittance. Langmuir **32**(3), 759–764 (2016)
29. Soler, J.M., et al.: The siesta method for ab initio order-n materials simulation. J. Phys.: Condens. Matter **14**(11), 2745 (2002)
30. Troullier, N., Martins, J.L.: Efficient pseudopotentials for plane-wave calculations. Phys. Rev. B **43**(3), 1993 (1991)
31. Perdew, J.P., Burke, K., Ernzerhof, M.: Generalized gradient approximation made simple. Phys. Rev. Lett. **77**(18), 3865 (1996)
32. Sommers, C., Doniach, S.: First principles calculation of the intra-atomic correlation energy in VO2. Solid State Commun. **28**(1), 133–135 (1978)
33. Dudarev, S.L., Botton, G.A., Savrasov, S.Y., Humphreys, C., Sutton, A.P.: Electron-energy-loss spectra and the structural stability of nickel oxide: an LSDA+U study. Phys. Rev. B **57**(3), 1505 (1998)
34. Kong, L., Lu, Y., Zhuang, X., Zhou, Z., Hu, Z.: Determining hubbard U of VO2 by the quasi-harmonic approximation. Chin. Phys. B **33**(1), 016302 (2024)
35. Longo, J.M., et al.: A refinement of the structure of VO2. Acta Chem. Scand. **24**(2), 420–426 (1970)
36. Eyert, V.: The metal-insulator transitions of VO2: a band theoretical approach. Annalen der Physik **514**(9), pp. 650–704 (2002)
37. McWhan, D., Marezio, M., Remeika, J., Dernier, P.: X-ray diffraction study of metallic VO2. Phys. Rev. B **10**(2), 490 (1974)
38. Cavalleri, A., et al.: Band-selective measurements of electron dynamics in VO2 using femtosecond near-edge X-Ray absorption. Phys. Rev. Lett. **95**(6), 067405 (2005)
39. Drude, P.: On the electron theory of metals. Ann. Phys. **1**, 566–613 (1900)
40. Allen, J., Mikkelsen, J.: Optical properties of CrSb, MnSb, NiSb, and NiAs. Phys. Rev. B **15**(6), 2952 (1977)
41. Smith, N.: Classical generalization of the Drude formula for the optical conductivity. Phys. Rev. B **64**(15), 155106 (2001)
42. Szymanski, N., Liu, Z., Alderson, T., Podraza, N., Sarin, P., Khare, S.: Electronic and optical properties of vanadium oxides from first principles. Comput. Mater. Sci. **146**, 310–318 (2018)
43. Ashok, P., Chauhan, Y.S., Verma, A.: High infrared reflectance modulation in VO2 films synthesized on glass and ITO coated glass substrates using atmospheric oxidation of vanadium. Opt. Mater. **110**, 110438 (2020)
44. Zhang, J., He, H., Xie, Y., Pan, B.: Theoretical study on the tungsten-induced reduction of transition temperature and the degradation of optical properties for VO2. J. Chem. Phys. **138**(11) (2013)